

Cosmological constraints on extended Galileon models

Antonio De Felice^{1,2} and Shinji Tsujikawa³

¹*TPTP & NEP, The Institute for Fundamental Study,
Naresuan University, Phitsanulok 65000, Thailand*

²*Thailand Center of Excellence in Physics, Ministry of Education, Bangkok 10400, Thailand*

³*Department of Physics, Faculty of Science, Tokyo University of Science,
1-3, Kagurazaka, Shinjuku-ku, Tokyo 162-8601, Japan*

(Dated: November 27, 2024)

The extended Galileon models possess tracker solutions with de Sitter attractors along which the dark energy equation of state is constant during the matter-dominated epoch, i.e. $w_{\text{DE}} = -1 - s$, where s is a positive constant. Even with this phantom equation of state there are viable parameter spaces in which the ghosts and Laplacian instabilities are absent. Using the observational data of the supernovae type Ia, the cosmic microwave background (CMB), and baryon acoustic oscillations, we place constraints on the tracker solutions at the background level and find that the parameter s is constrained to be $s = 0.034^{+0.327}_{-0.034}$ (95 % CL) in the flat Universe. In order to break the degeneracy between the models we also study the evolution of cosmological density perturbations relevant to the large-scale structure (LSS) and the Integrated-Sachs-Wolfe (ISW) effect in CMB. We show that, depending on the model parameters, the LSS and the ISW effect is either positively or negatively correlated. It is then possible to constrain viable parameter spaces further from the observational data of the ISW-LSS cross-correlation as well as from the matter power spectrum.

I. INTRODUCTION

The main target of the dark energy research over the next few years or so is to distinguish between the Λ -Cold-Dark-Matter (Λ CDM) model and dynamical models with time-varying equations of state w_{DE} . From the observational data of WMAP7 combined with baryon acoustic oscillations (BAO) [1] and the Hubble constant measurement [2], Komatsu *et al.* [3] derived the bound $w_{\text{DE}} = -1.10 \pm 0.14$ (68 % CL) for the constant equation of state. Adding the supernovae type Ia (SN Ia) data provides tighter constraints on w_{DE} , but still the phantom equation of state ($w_{\text{DE}} < -1$) is allowed by the joint data analysis [3]. This property persists for the time-varying dark energy equation of state with the parametrization such as $w_{\text{DE}} = w_0 + w_a(1 - a)$ [4], where a is the scale factor [5].

In the framework of General Relativity (GR) it is generally difficult to construct theoretically consistent models of dark energy which realize $w_{\text{DE}} < -1$. In quintessence [6] with a slowly varying scalar-field potential, for example, the field equation of state is always larger than -1 . A ghost field with a negative kinetic energy leads to $w_{\text{DE}} < -1$ [7], but such a field is plagued by a catastrophic instability of the vacuum associated with the spontaneous creation of ghost and photon pairs [8].

In modified gravitational theories it is possible to realize $w_{\text{DE}} < -1$ without having ghosts and Laplacian-type instabilities (see Refs. [9]). In $f(R)$ gravity, where the Lagrangian f is a function of the Ricci scalar R , the dark energy equation of state crosses the cosmological constant boundary ($w_{\text{DE}} = -1$) [10–13] for the viable models constructed to satisfy cosmological and local gravity constraints [10–12, 14]. This is also the case for the Brans-Dicke theory [15] with a field potential which accommodates the chameleon mechanism [16] to suppress the propagation of the fifth force [17]. In modified gravity models of dark energy based on the chameleon mechanism (including $f(R)$ gravity), the effective potential of a scalar degree of freedom needs to be carefully designed to pass cosmological and local gravity constraints [18].

There is another class of modified gravity models of dark energy in which a nonlinear self-interaction of a scalar degree of freedom ϕ can lead to the recovery of GR in a local region through the Vainshtein mechanism [19]. The representative models of this class are those based on the Dvali-Gabadadze-Porrati (DGP) braneworld [20] and the Galileon gravity [21] (see Refs. [22, 23] for the implementation of the Vainshtein mechanism in these models). The nonlinear interaction of the form $(\partial\phi)^2\Box\phi$, which appears from the brane-bending mode in the DGP model [22], gives rise to the field equation invariant under the Galilean shift $\partial_\mu\phi \rightarrow \partial_\mu\phi + b_\mu$ in the flat spacetime. This was extended to more general field Lagrangians satisfying the Galilean symmetry in the limit of the Minkowski spacetime [21, 24].

The cosmology based on the covariant Galileon or on its modified versions has been studied by many authors [25, 26]. In Refs. [27, 28] the dynamics of dark energy was investigated in the presence of the full covariant Galileon Lagrangian. In this model the solutions with different initial conditions converge to a common trajectory (tracker). Along the tracker the dark energy equation of state w_{DE} changes as $-7/3$ (radiation era) $\rightarrow -2$ (matter era) $\rightarrow -1$ (de Sitter era) [27–30]. There exists a viable parameter space in which the ghosts and Laplacian instabilities are absent. However, the joint analysis based on the observational data of SN Ia, CMB, and BAO shows that the tracker

solution is disfavored because of the large deviation of w_{DE} from -1 during the matter era [30, 31]. The solutions that approach the tracker only at late times are allowed from the combined data analysis [31].

As an extension of the covariant Galileon model, Deffayet *et al.* [32] obtained the most general Lagrangian in scalar-tensor theories with second-order equations of motion. In four dimensions the corresponding Lagrangian is of the form (1) with the four functions (2)-(5) given below. In fact this is equivalent to the Lagrangian found by Horndeski [33] more than 3 decades ago [34, 35]. The conditions for the avoidance of ghosts and Laplacian instabilities were recently derived in Ref. [36] in the presence of two perfect fluids (non-relativistic matter and radiation).

The covariant Galileon corresponds to the choice $K = -c_2 X$, $G_3 = c_3 X/M^3$, $G_4 = M_{\text{pl}}^2/2 - c_4 X^2/M^6$, $G_5 = 3c_5 X^2/M^9$ in Eqs. (2)-(5), where c_i 's are dimensionless constants, $X = -\partial^\mu \phi \partial_\mu \phi/2$, M_{pl} is the reduced Planck mass, and M is a constant having the dimension of mass. Kimura and Yamamoto [30] studied the model with the functions $K = -c_2 X$, $G_3 = c_3 M^{1-4n} X^n$ ($n \geq 1$), $G_4 = M_{\text{pl}}^2/2$, and $G_5 = 0$, in which case the dark energy equation of state during the matter era is given by $w_{\text{DE}} = -1 - s$ with $s = 1/(2n-1) > 0$. At the background level this is equivalent to the Dvali-Turner model [37], which can be consistent with the observational data for n larger than the order of 1. If we consider the evolution of cosmological perturbations, the LSS tends to be anti-correlated with the late-time ISW effect. This places the tight bound on the power n , as $n > 4.2 \times 10^3$ (95% CL) [38], in which case the dark energy equation of state is practically indistinguishable from that in the Λ CDM model.

In Ref. [36] the present authors proposed more general extended Galileon models with the functions $K = -c_2 M_2^{4(1-p_2)} X^{p_2}$, $G_3 = c_3 M_3^{1-4p_3} X^{p_3}$, $G_4 = M_{\text{pl}}^2/2 - c_4 M_4^{2-4p_4} X^{p_4}$, and $G_5 = 3c_5 M_5^{-(1+4p_5)} X^{p_5}$, where the masses M_i 's are fixed by the Hubble parameter at the late-time de Sitter solution with $\dot{\phi} = \text{constant}$. For the powers $p_2 = p$, $p_3 = p + (2q-1)/2$, $p_4 = p + 2q$, $p_5 = p + (6q-1)/2$, where p and q are positive constants, there exists a tracker solution characterized by $H\dot{\phi}^{2q} = \text{constant}$. During the matter-dominated epoch one has $w_{\text{DE}} = -1 - s$, where $s = p/(2q)$, along the tracker. This covers the model of Kimura and Yamamoto [30] as a specific case ($p = 1$, $q = n - 1/2$, $c_4 = 0$, $c_5 = 0$). In the presence of the nonlinear field self-interactions in G_4 and G_5 , the degeneracy of the background tracker solution for given values of p and q is broken by considering the evolution of cosmological perturbations. Hence the ISW-LSS anti-correlation found in Refs. [30, 38] for $c_4 = c_5 = 0$ should not be necessarily present for the models with non-zero values of c_4 and c_5 .

In this paper we first place constraints on the tracker solution in the extended Galileon models by using the recent observational data of SN Ia, CMB, and BAO. The bound on the value $s = p/(2q)$ is derived from the background cosmic expansion history with/without the cosmic curvature K . We then study the evolution of cosmological density perturbations in the presence of non-relativistic matter to break the degeneracy of the tracker solution at the background level. We will show that the LSS and the ISW effect are either positively or negatively correlated, depending on the parameters c_4 and c_5 . This information should be useful to distinguish between the extended Galileon models with different values of c_4 and c_5 from observations.

II. BACKGROUND FIELD EQUATIONS

We start with the following Lagrangian

$$\mathcal{L} = \sum_{i=2}^5 \mathcal{L}_i, \quad (1)$$

where

$$\mathcal{L}_2 = K(X), \quad (2)$$

$$\mathcal{L}_3 = -G_3(X) \square \phi, \quad (3)$$

$$\mathcal{L}_4 = G_4(X) R + G_{4,X} [(\square \phi)^2 - (\nabla_\mu \nabla_\nu \phi) (\nabla^\mu \nabla^\nu \phi)], \quad (4)$$

$$\mathcal{L}_5 = G_5(X) G_{\mu\nu} (\nabla^\mu \nabla^\nu \phi) - (G_{5,X}/6)[(\square \phi)^3 - 3(\square \phi) (\nabla_\mu \nabla_\nu \phi) (\nabla^\mu \nabla^\nu \phi) + 2(\nabla^\mu \nabla_\alpha \phi) (\nabla^\alpha \nabla_\beta \phi) (\nabla^\beta \nabla_\mu \phi)]. \quad (5)$$

K and G_i ($i = 3, 4, 5$) are functions in terms of the field kinetic energy $X = -\partial^\mu \phi \partial_\mu \phi/2$ with $G_{i,X} \equiv dG_i/dX$, R is the Ricci scalar, and $G_{\mu\nu}$ is the Einstein tensor. If we allow the ϕ -dependence for the functions K and G_i as well, the Lagrangian (1) corresponds to the most general Lagrangian in scalar-tensor theories [32, 33]. In order to discuss models relevant to dark energy we also take into account the perfect fluids of non-relativistic matter and radiation (with the Lagrangians \mathcal{L}_m and \mathcal{L}_r respectively), in which case the total 4-dimensional action is given by

$$S = \int d^4x \sqrt{-g} (\mathcal{L} + \mathcal{L}_m + \mathcal{L}_r). \quad (6)$$

In the following we focus on the extended Galileon models [36] in which K and G_i are given by

$$K = -c_2 M_2^{4(1-p_2)} X^{p_2}, \quad G_3 = c_3 M_3^{1-4p_3} X^{p_3}, \quad G_4 = M_{\text{pl}}^2/2 - c_4 M_4^{2-4p_4} X^{p_4}, \quad G_5 = 3c_5 M_5^{-(1+4p_5)} X^{p_5}, \quad (7)$$

where M_{pl} is the reduced Planck mass, c_i and p_i ($i = 2, 3, 4, 5$) are dimensionless constants, and M_i ($i = 2, 3, 4, 5$) are constants having the dimension of mass. In the flat Universe it was shown in Ref. [36] that tracker solutions characterized by the condition $H\dot{\phi}^{2q} = \text{constant}$ ($q > 0$ and a dot represents a derivative with respect to cosmic time t) are present for

$$p_2 = p, \quad p_3 = p + (2q - 1)/2, \quad p_4 = p + 2q, \quad p_5 = p + (6q - 1)/2. \quad (8)$$

The covariant Galileon [24] corresponds to $p = 1$ and $q = 1/2$, i.e. $p_2 = p_3 = 1$, $p_4 = p_5 = 2$.

We will extend the analysis to the general Friedmann-Lemaître-Robertson-Walker (FLRW) background with the cosmic curvature K :

$$ds^2 = -dt^2 + a^2(t) \left[\frac{dr^2}{1 - Kr^2} + r^2(d\theta^2 + \sin^2\theta d\phi^2) \right], \quad (9)$$

where $a(t)$ is the scale factor. The closed, flat, and open geometries correspond to $K > 0$, $K = 0$, and $K < 0$, respectively. For the theories given by the action (6) the dynamical equations of motion are

$$3H^2 M_{\text{pl}}^2 = \rho_{\text{DE}} + \rho_m + \rho_r + \rho_K, \quad (10)$$

$$(3H^2 + 2\dot{H})M_{\text{pl}}^2 = -P_{\text{DE}} - \rho_r/3 + \rho_K/3, \quad (11)$$

$$\dot{\rho}_m + 3H\rho_m = 0, \quad (12)$$

$$\dot{\rho}_r + 4H\rho_r = 0, \quad (13)$$

$$\dot{\rho}_K + 2H\rho_K = 0. \quad (14)$$

Here $H \equiv \dot{a}/a$, $\rho_K \equiv -3KM_{\text{pl}}^2/a^2$, ρ_m and ρ_r are the energy densities of non-relativistic matter and radiation respectively, and

$$\rho_{\text{DE}} \equiv 2XK_{,X} - K + 6H\dot{\phi}XG_{3,X} - 6H^2\tilde{G}_4 + 24H^2X(G_{4,X} + XG_{4,XX}) + 2H^3\dot{\phi}X(5G_{5,X} + 2XG_{5,XX}), \quad (15)$$

$$P_{\text{DE}} \equiv K - 2X\ddot{\phi}G_{3,X} + 2(3H^2 + 2\dot{H})\tilde{G}_4 - 4(3H^2X + H\dot{X} + 2\dot{H}X)G_{4,X} - 8HX\dot{X}G_{4,XX} - 2X(2H^3\dot{\phi} + 2H\dot{H}\dot{\phi} + 3H^2\ddot{\phi})G_{5,X} - 4H^2X^2\ddot{\phi}G_{5,XX}, \quad (16)$$

where $\tilde{G}_4 \equiv G_4 - M_{\text{pl}}^2/2 = -c_4 M_4^{2-4p_4} X^{p_4}$.

From Eqs. (10) and (11) we find that there exists a de Sitter solution characterized by $\dot{H} = 0$ and $\ddot{\phi} = 0$. In order to discuss the cosmological dynamics we introduce the dimensionless variables [36]

$$r_1 \equiv \left(\frac{x_{\text{dS}}}{x}\right)^{2q} \left(\frac{H_{\text{dS}}}{H}\right)^{1+2q}, \quad r_2 \equiv \left[\left(\frac{x}{x_{\text{dS}}}\right)^2 \frac{1}{r_1^3}\right]^{\frac{p+2q}{1+2q}}, \quad \Omega_r \equiv \frac{\rho_r}{3H^2 M_{\text{pl}}^2}, \quad (17)$$

where $x \equiv \dot{\phi}/(HM_{\text{pl}})$, and the subscript ‘‘dS’’ represents the quantities at the de Sitter solution. We relate the masses M_i ($i = 2, \dots, 5$) in Eq. (7) with H_{dS} , as $M_2 \equiv (H_{\text{dS}}M_{\text{pl}})^{1/2}$, $M_3 \equiv (H_{\text{dS}}^{-2p_3} M_{\text{pl}}^{1-2p_3})^{1/(1-4p_3)}$, $M_4 \equiv (H_{\text{dS}}^{-2p_4} M_{\text{pl}}^{2-2p_4})^{1/(2-4p_4)}$, and $M_5 \equiv (H_{\text{dS}}^{2+2p_5} M_{\text{pl}}^{2p_5-1})^{1/(1+4p_5)}$. The existence of de Sitter solutions demands that the coefficients c_2 and c_3 are related with c_4 and c_5 , via

$$c_2 = \frac{3}{2} \left(\frac{2}{x_{\text{dS}}^2}\right)^p (3\alpha - 4\beta + 2), \quad c_3 = \frac{\sqrt{2}}{2p+q-1} \left(\frac{2}{x_{\text{dS}}^2}\right)^{p+q} [3(p+q)(\alpha - \beta) + p], \quad (18)$$

where

$$\alpha \equiv \frac{4(2p_4 - 1)}{3} \left(\frac{x_{\text{dS}}^2}{2}\right)^{p_4} c_4, \quad \beta \equiv 2\sqrt{2}p_5 \left(\frac{x_{\text{dS}}^2}{2}\right)^{p_5+1/2} c_5. \quad (19)$$

The density parameter of dark energy, $\Omega_{\text{DE}} \equiv \rho_{\text{DE}}/(3H^2 M_{\text{pl}}^2)$, can be expressed as

$$\Omega_{\text{DE}} = \frac{r_1^{\frac{p-1}{2q+1}} r_2}{2} \left[r_1 \{ r_1 [12(\alpha - \beta)(p+q) + 4p - r_1(2p-1)(3\alpha - 4\beta + 2)] - 3\alpha(2p+4q+1) \} + 4\beta(p+3q+1) \right]. \quad (20)$$

From Eq. (10) it follows that $\Omega_{\text{DE}} + \Omega_m + \Omega_r + \Omega_K = 1$, where $\Omega_m \equiv \rho_m/(3H^2 M_{\text{pl}}^2)$ and $\Omega_K \equiv \rho_K/(3H^2 M_{\text{pl}}^2)$.

The autonomous equations for r_1 , r_2 , and Ω_r are written in terms of r_1 , r_2 , Ω_r , α , β , p , q . As in the case of the flat Universe [36] one can show that there is a fixed point for the differential equation of r_1 characterized by

$$r_1 = 1, \quad (21)$$

From the definition of r_1 in Eq. (17) this corresponds to the tracker solution where $H\dot{\phi}^{2q} = \text{constant}$. Along the tracker the autonomous equations for r_2 and Ω_r are

$$r_2' = \frac{(p+2q)(\Omega_r + 3 - 3r_2 - \Omega_K)}{pr_2 + 2q} r_2, \quad (22)$$

$$\Omega_r' = \frac{2q(\Omega_r - 1 - 3r_2 - \Omega_K) - 4pr_2}{pr_2 + 2q} \Omega_r, \quad (23)$$

where a prime represents the derivative with respect to $N = \ln a$. Combining these equations, we obtain the integrated solution

$$r_2 = c_1 a^{4(1+s)} \Omega_r^{1+s}, \quad s = \frac{p}{2q}, \quad (24)$$

where c_1 is a constant. For the theoretical consistency the parameter s is positive [36]. Since $r_2 \propto H^{-2(1+s)}$, the quantity r_2 grows toward the value 1 at the de Sitter solution. Along the tracker the density parameter (20) is given by

$$\Omega_{\text{DE}} = r_2 = \frac{1 - \Omega_{m,0} - \Omega_{r,0} - \Omega_{K,0}}{\Omega_{r,0}^{1+s}} e^{4(1+s)N} \Omega_r^{1+s}, \quad (25)$$

where the subscripts ‘‘0’’ represent the values today (the scale factor $a_0 = 1$, i.e. $N_0 = \ln a_0 = 0$). Using the relation $\Omega_K/\Omega_r = (\Omega_{K,0}/\Omega_{r,0})e^{2N}$ as well, Eq. (23) reads

$$\Omega_r' = -\frac{1 - \Omega_r + \Omega_{K,0}e^{2N} \Omega_r/\Omega_{r,0} + (1 - \Omega_{m,0} - \Omega_{r,0} - \Omega_{K,0})(3 + 4s) e^{4(1+s)N} \Omega_r^{1+s}/\Omega_{r,0}^{1+s}}{1 + (1 - \Omega_{m,0} - \Omega_{r,0} - \Omega_{K,0})s e^{4(1+s)N} \Omega_r^{1+s}/\Omega_{r,0}^{1+s}} \Omega_r. \quad (26)$$

This equation can be solved as

$$\frac{1 - \Omega_{m,0} - \Omega_{r,0} - \Omega_{K,0}}{\Omega_{r,0}^{1+s}} e^{4(1+s)N} \Omega_r^{1+s} + \frac{\Omega_{m,0}}{\Omega_{r,0}} e^N \Omega_r + \Omega_r + \frac{\Omega_{K,0}}{\Omega_{r,0}} e^{2N} \Omega_r = 1, \quad (27)$$

which is nothing but the relation $\Omega_{\text{DE}} + \Omega_m + \Omega_r + \Omega_K = 1$. From Eq. (25) the dark energy density parameter evolves as $\Omega_{\text{DE}} \propto H^{-2(1+s)}$ and hence

$$\frac{H}{H_0} = \left(\frac{\Omega_{\text{DE},0}}{\Omega_{\text{DE}}} \right)^{1/[2(1+s)]}. \quad (28)$$

Since it is not generally possible to solve Eq. (27) for Ω_r in terms of N (apart from some specific values of s such as $s = 1$), we numerically integrate Eq. (26) and find the expression of H/H_0 by using Eqs. (25) and (28).

Along the tracker the dark energy equation of state $w_{\text{DE}} \equiv P_{\text{DE}}/\rho_{\text{DE}}$ and the effective equation of state $w_{\text{eff}} \equiv -1 - 2\dot{H}/(3H^2)$ are given by

$$w_{\text{DE}} = -\frac{3 + s(3 + \Omega_r - \Omega_K)}{3(1 + sr_2)}, \quad w_{\text{eff}} = -\frac{r_2(3s + 3 - s\Omega_K) - \Omega_r}{3(1 + sr_2)}. \quad (29)$$

In the early cosmological epoch ($r_2 \ll 1$) these reduce to $w_{\text{DE}} \simeq -1 - s(3 + \Omega_r - \Omega_K)/3$ and $w_{\text{eff}} \simeq \Omega_r/3$. During the matter era in which $\{\Omega_r, |\Omega_K|\} \ll 1$ it follows that $w_{\text{DE}} \simeq -1 - s < -1$ (for $s > 0$) and $w_{\text{eff}} \simeq 0$. At the de Sitter fixed point ($r_2 = 1$) with $\Omega_r = \Omega_K = 0$ one has $w_{\text{DE}} = w_{\text{eff}} = -1$. In Fig. 1 we plot the evolution of w_{DE} versus the redshift $z = a_0/a - 1$ in the open Universe with $\Omega_{K,0} = 0.1$ for the model parameters $p = 1$, $q = 5/2$, $\alpha = 3$, $\beta = 1.45$ (i.e. $s = 0.2$). The tracker is shown as a solid curve, along which w_{DE} changes as -1.267 (radiation era) $\rightarrow -1.2$ (matter era) $\rightarrow -1$ (de Sitter era). The effect of the cosmic curvature Ω_K becomes important only for the late Universe, which affects the luminosity distance in the SN Ia observations.

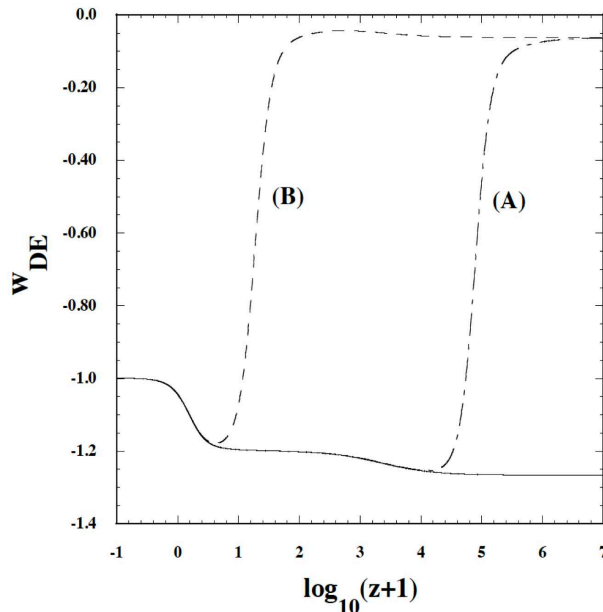


Figure 1. Evolution of w_{DE} versus the redshift z for the open Universe with $\Omega_{K,0} = 0.1$ for $p = 1$, $q = 5/2$, $\alpha = 3$, $\beta = 1.45$. The solid curve corresponds to the tracker solution with the initial conditions $r_1 = 1$, $r_2 = 1.0 \times 10^{-30}$, $\Omega_r = 0.99987$, $\Omega_K = 4.0 \times 10^{-12}$ at $\log_{10}(z+1) = 7.245$. In the cases (A) and (B) the initial conditions are chosen to be (A) $r_1 = 1.0 \times 10^{-2}$, $r_2 = 1.0 \times 10^{-23}$, $\Omega_r = 0.99985$, $\Omega_K = 5.0 \times 10^{-12}$ at $\log_{10}(z+1) = 7.210$, and (B) $r_1 = 3.0 \times 10^{-6}$, $r_2 = 1.0 \times 10^{-10}$, $\Omega_r = 0.9998$, $\Omega_K = 1.15 \times 10^{-11}$ at $\log_{10}(z+1) = 6.967$, respectively.

If the solutions start from the regime $r_1 \ll 1$, the evolution of w_{DE} is different from Eq. (29) before they reach the tracker. For $r_1 \ll 1$ and $r_2 \ll 1$, w_{DE} and w_{eff} are approximately given by

$$w_{\text{DE}} \simeq -\frac{1 + \Omega_r - \Omega_K}{2(2p + 6q - 1)}, \quad w_{\text{eff}} \simeq \frac{1}{3}\Omega_r. \quad (30)$$

In Fig. 1 we show the variation of w_{DE} for $p = 1$, $q = 5/2$, $\alpha = 3$, $\beta = 1.45$ with two different initial conditions satisfying $r_1 \ll 1$. In both cases the density parameter Ω_K today is $\Omega_{K,0} = 0.1$. The cases (A) and (B) correspond to the early and late trackings, respectively. For smaller initial values of r_1 the tracking occurs later. As estimated by Eq. (30), w_{DE} starts from the value $w_{\text{DE}} \simeq -1/16$ in the deep radiation era. If the solutions do not reach the tracker during the matter era (as in the case (B) in Fig. 1), w_{DE} temporally approaches the value $-1/32$.

In Ref. [31] it was shown that the tracker for the covariant Galileon ($s = 1$) is disfavored from observations, but the late-time tracking solution is allowed from the data. This property comes from the fact that for the late-time tracker the deviation of w_{DE} from -1 is not significant. For $s \ll 1$ even the tracker is expected to be allowed from observations. In such cases the solutions starting from the initial conditions with $r_1 \ll 1$ should be also compatible with the data (because even for $s = 1$ the late-time tracking solution is allowed). In the following sections we will focus on the tracker solution to discuss the background observational constraints and the evolution of cosmological perturbations.

III. OBSERVATIONAL CONSTRAINTS ON THE EXTENDED GALILEON MODELS

In this section we place observational constraints on the tracker solution from the background cosmic expansion history. We use three data sets: 1) the CMB shift parameters (WMAP7) [3]; 2) the BAO (SDSS7) [1]; 3) and the SN Ia (Constitution) [39]. The total chi-square χ_{tot}^2 for all three combined data sets will be calculated on a grid representing a chosen set of available parameters. We then find the minimum on this grid, and consequently find the 1σ and 2σ contours.

In order to integrate Eq. (26), once a set of model parameters (in this case not only s , but also $\Omega_{r,0}$, $\Omega_{m,0}$, and $\Omega_{K,0}$) is given, we have the choice of one initial condition, that is $\Omega_{r,i} \equiv \Omega_r(N_i)$. In principle it is possible to solve Eq. (26) backwards for a given value of $\Omega_r(0) = \Omega_{r,0}$, but we find that the integrated results are prone to numerical instabilities.

Therefore, it is more convenient to obtain the expression of $\Omega_{r,i}$ for a given $N_i < 0$ (chosen to be $N_i = -\ln(1+z_i)$, where the initial redshift is $z_i = 1.76 \times 10^7$), which gives $\Omega_r(N=0) = \Omega_{r,0}$ after solving the differential equation.

For given $\Omega_{r,0}$ and the other parameters we can use Eq. (27) to obtain the desired value of $\Omega_{r,i}$. At $N = N_i$, Eq. (27) is written as

$$\left(1 + \frac{\Omega_{K,0}}{\Omega_{r,0}} e^{2N_i} + \frac{\Omega_{m,0}}{\Omega_{r,0}} e^{N_i}\right) \Omega_{r,i} - 1 = -\frac{1 - \Omega_{m,0} - \Omega_{K,0} - \Omega_{r,0}}{\Omega_{r,0}^{1+s}} e^{4(1+s)N_i} \Omega_{r,i}^{1+s}. \quad (31)$$

Since $\Omega_{r,i} \approx 1$ during the radiation domination, it is possible to solve this equation iteratively by assuming that the l.h.s. is a small correction (indeed the r.h.s. corresponds to $-\Omega_{\text{DE},i}$). At 0-th order the solution of Eq. (31) is given by

$$\Omega_{r,i}^{(0)} = \frac{1}{1 + (\Omega_{K,0}/\Omega_{r,0}) e^{2N_i} + (\Omega_{m,0}/\Omega_{r,0}) e^{N_i}}. \quad (32)$$

At first order we find

$$\Omega_{r,i}^{(1)} = \frac{1 - (1 - \Omega_{m,0} - \Omega_{K,0} - \Omega_{r,0}) e^{4(1+s)N_i} [\Omega_{r,i}^{(0)}/\Omega_{r,0}]^{1+s}}{1 + (\Omega_{K,0}/\Omega_{r,0}) e^{2N_i} + (\Omega_{m,0}/\Omega_{r,0}) e^{N_i}}. \quad (33)$$

This process can be iterated up to the desired precision. In the numerical code, we employ the solution derived after the three iterations, that is $\Omega_{r,i} \simeq \Omega_{r,i}^{(3)}$. Since the late-time de Sitter background is an attractor, small differences in the initial conditions do not lead to very different final solutions. Therefore we indeed find that the three iterations are sufficient to derive the parameter $\Omega_{r,0}$ accurately.

In the following we first discuss the method for carrying out the likelihood analysis to confront the tracker solution with observations and then proceed to constrain the model parameters.

A. CMB shift parameters

We use the data of the CMB shift parameters provided by WMAP7, which are related with the positions of the CMB acoustic peaks. These quantities are affected by the cosmic expansion history from the decoupling epoch to today. The redshift at the decoupling is known by means of the fitting formula of Hu and Sugiyama [40]

$$z_* = 1048 [1 + 0.00124(\Omega_{b,0}h^2)^{-0.738}] [1 + g_1 (\Omega_{m,0}h^2)^{g_2}], \quad (34)$$

where $g_1 = 0.0783 (\Omega_{b,0}h^2)^{-0.238} / [1 + 39.5 (\Omega_{b,0}h^2)^{0.763}]$, $g_2 = 0.560 / [1 + 21.1 (\Omega_{b,0}h^2)^{1.81}]$, $h = H_0 / [100 \text{ km sec}^{-1} \text{ Mpc}^{-1}]$, and $\Omega_{b,0}$ corresponds to the today's density parameter of baryons. The shift of the CMB acoustic peaks can be quantified by the two shift parameters [41]

$$\mathcal{R} = \sqrt{\frac{\Omega_{m,0}}{\Omega_{K,0}}} \sinh \left(\sqrt{\Omega_{K,0}} \int_0^{z_*} \frac{dz}{H(z)/H_0} \right), \quad l_a = \frac{\pi d_a^{(c)}(z_*)}{r_s(z_*)}, \quad (35)$$

where $r_s(z_*)$ corresponds to the sound horizon at the decoupling, given by

$$r_s(z_*) = \int_{z_*}^{\infty} \frac{dz}{H(z) \sqrt{3\{1 + 3\Omega_{b,0}/[4\Omega_{\gamma,0}(1+z)]\}}}. \quad (36)$$

Note that $\Omega_{\gamma,0}$ is the today's value of photon energy density and $d_a^{(c)}(z_*)$ is the comoving angular distance to the last scattering surface defined by $d_a^{(c)}(z_*) = \mathcal{R}/[H_0\sqrt{\Omega_{m,0}}]$.

The likelihood values of l_a, \mathcal{R}, z_* provided by the WMAP7 data [3] are $l_a = 302.09 \pm 0.76$, $\mathcal{R} = 1.725 \pm 0.018$, and $z_* = 1091.3 \pm 0.91$. The chi-square associated with this measurement is

$$\chi_{\text{CMB}}^2 = (l_a - 302.09, \mathcal{R} - 1.725, z_* - 1091.3) \mathbf{C}_{\text{CMB}}^{-1} \begin{pmatrix} l_a - 302.09 \\ \mathcal{R} - 1.725 \\ z_* - 1091.3 \end{pmatrix}, \quad (37)$$

where the inverse covariance matrix is

$$\mathbf{C}_{\text{CMB}}^{-1} = \begin{pmatrix} 2.305 & 29.698 & -1.333 \\ 29.698 & 6825.27 & -113.18 \\ -1.333 & -113.18 & 3.414 \end{pmatrix}. \quad (38)$$

B. BAO

We also employ the data of BAO measured by the SDSS7 [1]. The redshift z_d at which the baryons are released from the Compton drag of photons is given by the fitting formula of Eisenstein and Hu [42]:

$$z_d = \frac{1291 (\Omega_{m,0} h^2)^{0.251}}{1 + 0.659 (\Omega_{m,0} h^2)^{0.828}} [1 + b_1 (\Omega_{b,0} h^2)^{b_2}], \quad (39)$$

where $b_1 = 0.313 (\Omega_{m,0} h^2)^{-0.419} [1 + 0.607 (\Omega_{m,0} h^2)^{0.674}]$ and $b_2 = 0.238 (\Omega_{m,0} h^2)^{0.223}$. We define the effective BAO distance

$$D_V(z) = [d_A^2(z) (1+z)^2 z / H(z)]^{1/3}, \quad (40)$$

where $d_A(z)$ is the diameter distance given by

$$d_A(z) = \frac{1}{1+z} \frac{1}{H_0 \sqrt{\Omega_{K,0}}} \sinh \left[\sqrt{\Omega_{K,0}} \int_0^z \frac{d\tilde{z}}{H(\tilde{z})/H_0} \right]. \quad (41)$$

The BAO observations constrain the ratio $r_s(z_d)/D_V(z)$ at particular redshifts z , where $r_s(z_d)$ is the sound horizon for $z = z_d$. At $z = 0.2$ and $z = 0.35$ the recent observational bounds are $r_s(z_d)/D_V(0.2) = 0.1905 \pm 0.0061$ and $r_s(z_d)/D_V(0.35) = 0.1097 \pm 0.0036$. The chi-square associated with the BAO is evaluated as

$$\chi_{\text{BAO}}^2 = (r_s(z_d)/D_V(0.2) - 0.1905, r_s(z_d)/D_V(0.35) - 0.1097) \mathbf{C}_{\text{BAO}}^{-1} \begin{pmatrix} r_s(z_d)/D_V(0.2) - 0.1905 \\ r_s(z_d)/D_V(0.35) - 0.1097 \end{pmatrix}, \quad (42)$$

where the inverse covariance matrix is [1]

$$\mathbf{C}_{\text{BAO}}^{-1} = \begin{pmatrix} 30124 & -17227 \\ -17227 & 86977 \end{pmatrix}. \quad (43)$$

C. SN Ia

Finally we consider the experimental bounds coming from the observations of the SN Ia standard candles. The apparent magnitudes, together with their absolute magnitudes, can be used to generate the following chi-square [43]

$$\chi_{\text{SN Ia}}^2 = \sum_i \frac{\mu_{\text{obs}}(z_i) - \mu_{\text{th}}(z_i)}{\sigma_{\mu,i}^2}, \quad (44)$$

where $\sigma_{\mu,i}^2$ are the errors on the data, and μ_{th} is the theoretical distance modulus defined as

$$\mu_{\text{th}}(z_i) = 5 \log_{10} [\bar{d}_L(z_i)] + \mu_0. \quad (45)$$

Here $\bar{d}_L(z)$ and μ_0 are given, respectively, by

$$\bar{d}_L(z) = (1+z)^2 H_0 d_A(z), \quad \mu_0 = 42.38 - 5 \log_{10} h. \quad (46)$$

In the following we will make use of the Constitution SN Ia data sets provided in Ref. [39] (see also Ref. [44]).

D. Observational constraints on the tracker

We now define the total chi-square as

$$\chi^2 = \chi_{\text{CMB}}^2 + \chi_{\text{BAO}}^2 + \chi_{\text{SN Ia}}^2. \quad (47)$$

In the following we reduce the numerical complexity by fixing several parameters, as $h = 0.71$, $\Omega_{b,0} = 0.02258 h^2$, $\Omega_{\gamma,0} = 2.469 \times 10^{-5} h^{-2}$, and $\Omega_{r,0} = \Omega_{\gamma,0} (1 + 0.2271 \mathcal{N}_{\text{eff}})$ [3], where the relativistic degrees of freedom are set to be $\mathcal{N}_{\text{eff}} = 3.04$. Then two analysis will be performed for the tracker solution: 1) the flat case, $\Omega_{K,0} = 0$, for which two

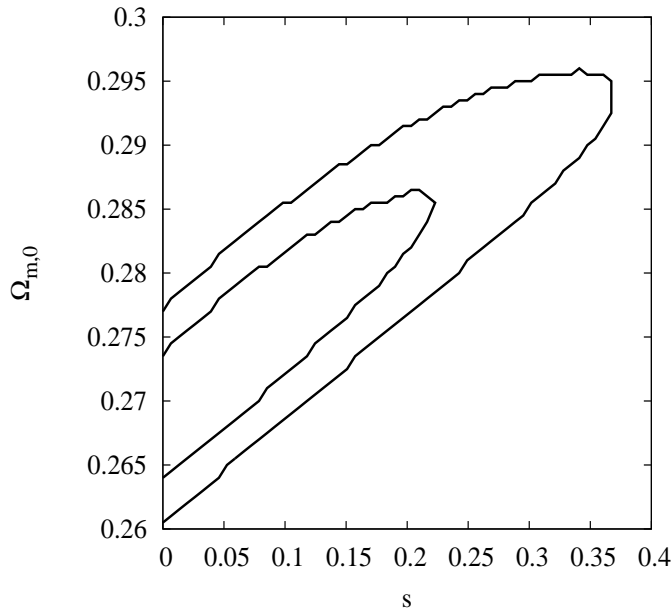


Figure 2. Observational contours for the tracker solution in the $(s, \Omega_{m,0})$ plane for the flat Universe ($\Omega_{K,0} = 0$). 1σ and 2σ contours correspond to the internal and external lines, respectively.

free parameters, $\Omega_{m,0}$ and s , are left to be varied; 2) the non-flat case, for which the additional free parameter, $\Omega_{K,0}$, is varied as well.

Later on, when we compare models with different number of free parameters, we will also make use of the Akaike Information Criterion (AIC) method (see e.g., [45]). For each model the AIC is defined as

$$\text{AIC} = \chi_{\min}^2 + 2\mathcal{P}, \quad (48)$$

where \mathcal{P} is the number of free parameters in the model, and χ_{\min}^2 is the minimum value for χ^2 in the chosen parameter space. The smaller the AIC the better the model. To be more precise, if the difference of χ^2 between two different models is in the range $0 < \Delta(\text{AIC}) < 2$, the models are considered to be equivalent, whereas if $\Delta(\text{AIC}) > 2$, the data prefer one model with respect to the other.

1. Flat case: $\Omega_{K,0} = 0$

In this case we compute the χ^2 on a grid in the intervals $0 \leq s < 0.9$ and $0.25 < \Omega_{m,0} < 0.32$. The minimum value of χ^2 is found to be $\chi_{\min}^2 = 468.876$ for the model parameters $s = 0.03446$ and $\Omega_{m,0} = 0.27159$. Then we calculate the difference of χ^2 at each grid point, that is, $\Delta\chi^2 = \chi^2 - \chi_{\min}^2$. When $\Delta\chi^2 \geq 2.88$ the chi-square distribution, with two free parameters, excludes the models with those values of χ^2 at 68% confidence level (1σ), whereas when $\Delta\chi^2 \geq 5.99$ those models are excluded at 95% CL (2σ).

Our numerical results are plotted in Fig. 2. Even if we use the Gaussian likelihood function $P \propto e^{-\chi^2/2}$, we find that the observational contours are similar to those given in Fig. 2. The parameters s and $\Omega_{m,0}$ are constrained to be

$$s = 0.034_{-0.034}^{+0.327}, \quad \Omega_{m,0} = 0.271_{-0.010}^{+0.024} \quad (95\% \text{ CL}). \quad (49)$$

This shows that the tracker solution with $-1.36 < w_{\text{DE}} < -1$ during the matter era can be allowed observationally. The Λ CDM model corresponds to the line $s = 0$ in Fig. 2, which, as expected, is inside the 1σ contour for $0.264 < \Omega_{m,0} < 0.273$ (with $\chi_{\Lambda\text{CDM}}^2 = 469.024$). The best-fit χ^2 for the extended Galileon model is slightly smaller than that in the Λ CDM model. However, since $\Delta(\text{AIC}) = 1.85$, the observational data do not particularly favor the extended Galileon model over the Λ CDM model.

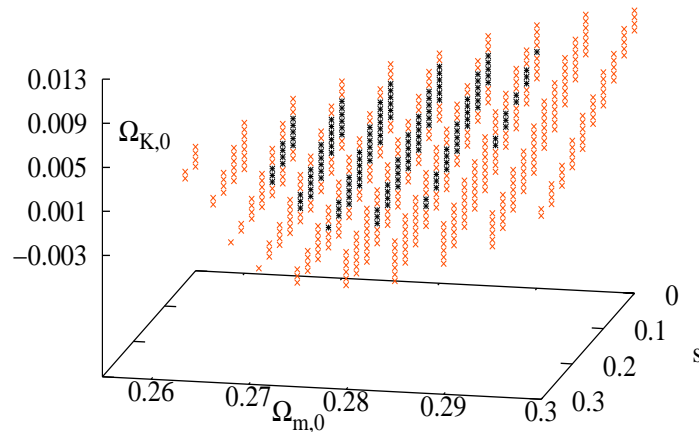


Figure 3. Observational contours for the tracker solution in the $(s, \Omega_{m,0}, \Omega_{K,0})$ space with the cosmic curvature taken into account. 1σ and 2σ contours correspond to the black and red regions, respectively.

2. Non-flat case: $\Omega_{K,0} \neq 0$

In the presence of the cosmic curvature K we also evaluate the χ^2 in the parameter space given by $0 \leq s < 0.9$, $0.25 < \Omega_{m,0} < 0.32$, and $-0.006 < \Omega_{K,0} < 0.014$. The minimum value of χ^2 is found on the point $s = 0.067$, $\Omega_{m,0} = 0.2768$, and $\Omega_{K,0} = 0.00768$, at which $\chi_{\min,K}^2 = 467.436$. We evaluate the difference $\Delta\chi_K^2 \equiv \chi^2 - \chi_{\min,K}^2$ on each grid point, according to which we can exclude: a) the values of χ^2 at 68% CL (which, for a system with 3 parameters, corresponds to $\Delta\chi_K^2 > 3.51$), and b) the values of χ^2 at 95% CL (i.e. $\Delta\chi_K^2 > 7.82$). In Fig. 3 we plot a three dimensional region (by showing only some slices of it) of the allowed parameter space for the tracker solution. We find that the model parameters are constrained to be

$$s = 0.067_{-0.067}^{+0.333}, \quad \Omega_{m,0} = 0.277_{-0.022}^{+0.023}, \quad \Omega_{K,0} = 0.0077_{-0.0127}^{+0.0039} \quad (95\% \text{ CL}). \quad (50)$$

The AIC for the best-fit extended Galileon model is $\text{AIC} = 473.436$, whereas in the best-fit ΛCDM model with two parameters $\Omega_{m,0}$ and $\Omega_{K,0}$ the AIC is found to be $\text{AIC}_{\Lambda\text{CDM},K} = 472.543$ with $\chi_{\Lambda\text{CDM},K}^2 = 468.543$. Since $\Delta(\text{AIC}) = 0.893$ between the two models, they are equivalently supported by the data. However, if we compare the non-flat extended Galileon model with the flat ΛCDM (1 parameter only, $\Omega_{m,0}$), then we see that $\Delta(\text{AIC}) = 2.412$, which states that the flat ΛCDM is better supported by the data. According to this criterion, the flat extended Galileon tracker is favored over the non-flat case from a statistical point of view.

IV. COSMOLOGICAL PERTURBATIONS AND THE DISCRIMINATION BETWEEN THE MODELS

The property of the tracker solution does not depend on the parameters α and β at the level of the background cosmology. If we consider cosmological perturbations, it is possible to discriminate between the models with different values of α and β . In order to confront the extended Galileon models with the observations of LSS, CMB, and weak lensing, we shall study the evolution of matter density perturbations as well as gravitational potentials. Since our interest is the growth of non-relativistic matter perturbations in the late Universe, we do not take into account the radiation as far as the perturbations are concerned.

A. Linear perturbation equations

Let us consider the perturbed metric in the longitudinal gauge about the flat FLRW background [46]

$$ds^2 = -(1 + 2\Psi) dt^2 + a^2(t)(1 + 2\Phi)\delta_{ij}dx^i dx^j, \quad (51)$$

where Ψ and Φ are scalar metric perturbations. We perturb the scalar field as $\phi(t) + \delta\phi(t, \mathbf{x})$, and non-relativistic matter as well, in terms of the matter density perturbation $\delta\rho_m$ and the scalar part of the fluid velocity v . The density contrast of non-relativistic matter is defined as $\delta \equiv \delta\rho_m/\rho_m$. We also introduce the gauge-invariant density contrast

$$\delta_m \equiv \delta + 3Hv. \quad (52)$$

The full linear perturbation equations in the Horndeski's most general scalar-tensor theories were derived in Ref. [47]. For the extended Galileon models, in Fourier space, they are given by

$$A_1\dot{\Phi} + A_2\dot{\delta}\phi - \rho_m\Psi + A_3\frac{k^2}{a^2}\Phi + A_4\Psi + A_6\frac{k^2}{a^2}\delta\phi - \rho_m\delta = 0, \quad (53)$$

$$B_6\Phi + B_7\delta\phi + A_3\Psi = 0, \quad (54)$$

$$A_3\dot{\Phi} + A_6\dot{\delta}\phi - A_1\Psi/3 + C_4\delta\phi + \rho_mv = 0, \quad (55)$$

$$3A_6\ddot{\Phi} + D_2\ddot{\delta}\phi + D_3\dot{\Phi} + D_4\dot{\delta}\phi - A_2\dot{\Psi} + \left(B_7\frac{k^2}{a^2} + D_8\right)\Phi + D_9\frac{k^2}{a^2}\delta\phi + \left(A_6\frac{k^2}{a^2} + D_{11}\right)\Psi = 0, \quad (56)$$

$$\dot{v} - \Psi = 0, \quad (57)$$

$$\dot{\delta} + 3\dot{\Phi} + \frac{k^2}{a^2}v = 0, \quad (58)$$

where k is a comoving wave number, and

$$A_1 = 12HG_4 - 6\dot{\phi}XG_{3,X} - 48HX(G_{4,X} + XG_{4,XX}) - 6H^2X(5G_{5,X} + 2XG_{5,XX})\dot{\phi}, \quad (59)$$

$$A_2 = -(K_{,X} + 2XK_{,XX})\dot{\phi} - 6HX(3G_{3,X} + 2XG_{3,XX}) - 6H^2(3G_{4,X} + 12XG_{4,XX} + 4X^2G_{4,XXX})\dot{\phi} - 2H^3X(15G_{5,X} + 20XG_{5,XX} + 4X^2G_{5,XXX}), \quad (60)$$

$$A_3 = 4G_4 - 8XG_{4,X} - 4H\dot{\phi}XG_{5,X}, \quad (61)$$

$$A_4 = 2X(K_{,X} + 2XK_{,XX}) - 12H^2G_4 + \rho_m + 12HX(2G_{3,X} + XG_{3,XX})\dot{\phi} + 12H^2X(7G_{4,X} + 16XG_{4,XX} + 4X^2G_{4,XXX}) + 4H^3X(15G_{5,X} + 13XG_{5,XX} + 2X^2G_{5,XXX})\dot{\phi}, \quad (62)$$

$$A_6 = -2XG_{3,X} - 4H(G_{4,X} + 2XG_{4,XX})\dot{\phi} - 2H^2X(3G_{5,X} + 2XG_{5,XX}), \quad (63)$$

$$B_6 = 4G_4 - 4XG_{5,X}\ddot{\phi}, \quad (64)$$

$$B_7 = -4G_{4,X}H\dot{\phi} - 4(G_{4,X} + 2XG_{4,XX})\ddot{\phi} - 4(G_{5,X} + XG_{5,XX})H\dot{\phi}\ddot{\phi} - 4XG_{5,X}(H^2 + \dot{H}), \quad (65)$$

$$C_4 = K_{,X}\dot{\phi} + 6HXG_{3,X} + 6H^2(G_{4,X} + 2XG_{4,XX})\dot{\phi} + 2XH^3(3G_{5,X} + 2XG_{5,XX}), \quad (66)$$

$$D_9 = -K_{,X} - 2(G_{3,X} + XG_{3,XX})\ddot{\phi} - 4HG_{3,X}\dot{\phi} - 4H(3G_{4,XX} + 2XG_{4,XXX})\dot{\phi}\ddot{\phi} - 2G_{4,X}(3H^2 + 2\dot{H}) - 4XG_{4,XX}(5H^2 + 2\dot{H}) - 2H^2(G_{5,X} + 5XG_{5,XX} + 2X^2G_{5,XXX})\ddot{\phi} - 4H(H^2 + \dot{H})(G_{5,X} + XG_{5,XX})\dot{\phi}. \quad (67)$$

The readers may refer to the paper [47] for the explicit forms of the coefficients D_2, D_3, D_4, D_8 , and D_{11} . Since the perturbation equations (53)-(58) are not independent, we do not need to know these unwritten coefficients to solve the equations numerically. Now we are dealing with a massless scalar field, so that the mass term M does not appear in the perturbation equations.

From Eqs. (57) and (58) the gauge-invariant matter perturbation (52) obeys

$$\ddot{\delta}_m + 2H\dot{\delta}_m + \frac{k^2}{a^2}\Psi = 3\left(\ddot{I} + 2H\dot{I}\right), \quad (68)$$

where $I \equiv Hv - \Phi$. We define the effective gravitational potential

$$\Phi_{\text{eff}} \equiv (\Psi - \Phi)/2. \quad (69)$$

This quantity is related to the deviation of the light rays in CMB and weak lensing observations [48]. To quantify the difference between the two gravitational potentials Φ and Ψ , we also introduce

$$\eta \equiv -\Phi/\Psi, \quad (70)$$

by which Eq. (69) can be written as $\Phi_{\text{eff}} = \Psi(1 + \eta)/2$.

B. Quasi-static approximation on sub-horizon scales

For the modes deep inside the Hubble radius ($k^2/a^2 \gg H^2$) we can employ the quasi-static approximation under which the dominant contributions in the perturbation equations are those including k^2/a^2 and δ (or δ_m) [49, 50]. This approximation is known to be trustable as long as the oscillating mode of the field perturbation is negligible relative to the matter-induced mode. Combining Eqs. (53), (54), and (56) under this approximation, it follows that [47]

$$\frac{k^2}{a^2}\Psi \simeq -4\pi G_{\text{eff}}\rho_m\delta, \quad (71)$$

where

$$G_{\text{eff}} = \frac{2M_{\text{pl}}^2(B_6D_9 - B_7^2)}{A_6^2B_6 + A_3^2D_9 - 2A_3A_6B_7}G. \quad (72)$$

Here we introduced the bare gravitational constant $G = 1/(8\pi M_{\text{pl}}^2)$. Substituting Eq. (71) into Eq. (68) with the relation $\delta_m \simeq \delta$ (valid for $k^2/a^2 \gg H^2$), we obtain

$$\delta_m'' + \left(2 + \frac{H'}{H}\right)\delta_m' - \frac{3}{2}\frac{G_{\text{eff}}}{G}\Omega_m\delta_m \simeq 0, \quad (73)$$

where a prime represents a derivative with respect to $N = \ln a$.

Under the quasi-static approximation the quantity η defined in Eq. (70) reads [47]

$$\eta \simeq \frac{A_3D_9 - A_6B_7}{B_6D_9 - B_7^2}. \quad (74)$$

On using Eq. (71), the effective gravitational potential $\Phi_{\text{eff}} = \Psi(1 + \eta)/2$ yields

$$\Phi_{\text{eff}} \simeq -\frac{3}{2}\xi \left(\frac{aH}{k}\right)^2 \Omega_m\delta_m, \quad (75)$$

where

$$\xi \equiv \frac{G_{\text{eff}}}{G} \frac{1 + \eta}{2} \simeq \frac{M_{\text{pl}}^2(B_6D_9 - B_7^2 + A_3D_9 - A_6B_7)}{A_6^2B_6 + A_3^2D_9 - 2A_3A_6B_7}. \quad (76)$$

The Λ CDM model corresponds to $K = -\Lambda$, $G_4 = M_{\text{pl}}^2/2$, $G_3 = G_5 = 0$, in which case $A_3 = B_6 = 2M_{\text{pl}}^2$, $A_6 = 0$, and $B_7 = 0$. Then one has $G_{\text{eff}}/G = 1$ and $\xi = 1$ from Eqs. (72) and (76).

In the extended Galileon models the general expressions of G_{eff}/G and ξ are quite complicated. In what follows we shall focus on the evolution of cosmological perturbations for the tracker solution ($r_1 = 1$).

In the early cosmological epoch ($r_2 \ll 1$) and during the matter domination ($\Omega_r = 0$), G_{eff}/G and ξ are approximately given by

$$\begin{aligned} G_{\text{eff}}/G \simeq & 1 + [27p(2p-1)(3\alpha^2p + 6\beta^2(2p-1) + \beta(1+3\alpha-2(1+6\alpha)p)) + 9(6\alpha^2p(18p-5) \\ & + 2\beta(2p-1)(\beta(90p-3) - 11p) + \alpha(2p(2p-1) - 3\beta(1+4p(33p-13))))]q + 2(-9(9\alpha-23\beta)(\alpha-2\beta) \\ & + 6(147\alpha^2 + \alpha(5-507\beta) + 6\beta(71\beta-3))p + 8(9\alpha-18\beta-1)p^2 + 16p^3q^2 + 4(9(27\alpha-46\beta)(\alpha-2\beta) \\ & - 12(9\alpha-18\beta-8)(\alpha-2\beta)p + 16(1-3\alpha+6\beta)p^2)q^3 + 48(\alpha-2\beta)(6\beta(7-2p) - 8p + 3\alpha(2p-7))q^4 \\ & + 576(\alpha-2\beta)^2q^5]r_2/\Delta, \end{aligned} \quad (77)$$

$$\begin{aligned} \xi \simeq & 1 + [27p(2p-1)(3\alpha^2p + 6\beta^2(2p-1) + \beta(1+3\alpha-2(1+6\alpha)p)) + 9(24\alpha^2p(4p-1) \\ & + 2\beta(2p-1)(\beta(78p+3) - 11p) + \alpha(4p(2p-1) + \beta(3+12(10-29p)p))]q + 2(-45(\alpha-2\beta)\beta \\ & + 6(96\alpha^2 + \alpha(10-321\beta) + 6\beta(43\beta-2))p + 4(27\alpha-54\beta-4)p^2 + 32p^3q^2 + 8(9(3\alpha-10\beta)(\alpha-2\beta) \\ & - 3(27\alpha-54\beta-26)(\alpha-2\beta)p + 16(1-3\alpha+6\beta)p^2)q^3 + 48(\alpha-2\beta)(66\beta-8(2+3\beta)p + 3\alpha(4p-11))q^4 \\ & + 1152(\alpha-2\beta)^2q^5]r_2/(2\Delta), \end{aligned} \quad (78)$$

where

$$\begin{aligned} \Delta \equiv & 4q[(3-9\alpha)p + 12p^3 + 2pq(\alpha(60-66q) + 20q-11) + 2p^2(\alpha(9-18q) + 22q-6) - 3\alpha q(9-54q+40q^2) \\ & + 3\beta(2p+4q-1)(3-22q+20q^2+6p(2q-1))]. \end{aligned} \quad (79)$$

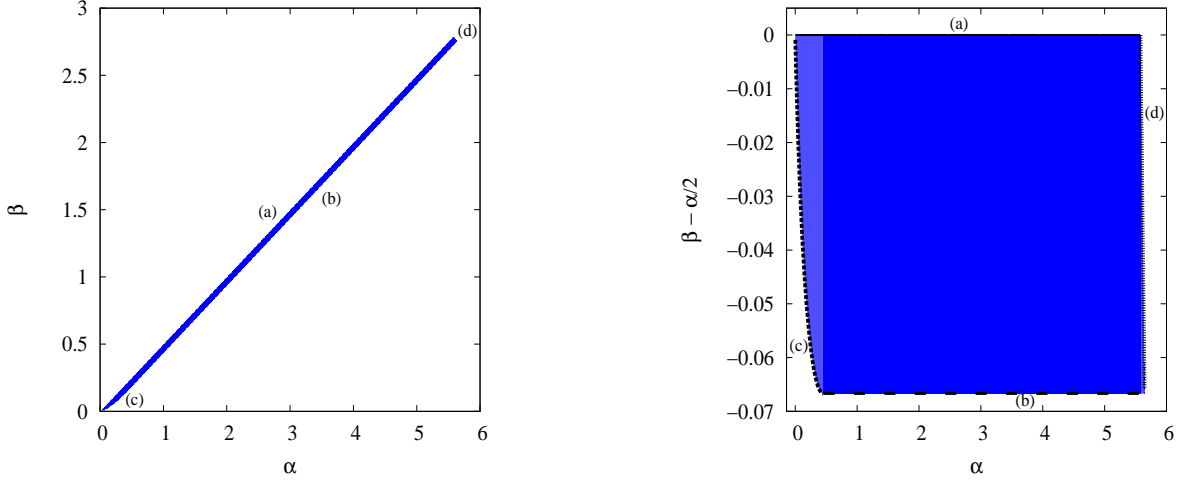


Figure 4. Allowed parameter space in the (α, β) plane for $p = 1$ and $q = 5/2$. In the blue region the conditions for the avoidance of ghosts and Laplacian instabilities of scalar and tensor perturbations are satisfied. The right panel shows the enlarged version of the left panel in the $(\alpha, \beta - \alpha/2)$ plane. The borders correspond to (a) $\beta = \alpha/2$, (b) $\beta = \alpha/2 - 1/15$, (c) $\beta = (408\alpha + 68 - 2\sqrt{17}\sqrt{3(272 - 75\alpha)\alpha + 68})/561$, and (d) $\beta = (242 - 15\alpha + 4\sqrt{3630 - 495\alpha})/99$, respectively. Taken from Ref. [36].

To derive Eqs. (77) and (78) we set $\Omega_r = 0$ and performed the Taylor expansion around $r_2 = 0$.

At the de Sitter solution ($r_1 = r_2 = 1$), G_{eff} and ξ are simply given by

$$G_{\text{eff}}/G = \xi = \frac{2}{2(1-p) + 3(1+2q)(\alpha - 2\beta)}. \quad (80)$$

The equality of G_{eff}/G and ξ comes from the fact that $\eta = 1$ at $r_1 = r_2 = 1$.

Let us first consider the theory where $\alpha = \beta = 0$. From Eqs. (77)-(80) it follows that

$$G_{\text{eff}}/G = \xi \simeq 1 + \frac{4pq}{6p + 10q - 3} r_2 \quad (\text{for } r_2 \ll 1), \quad (81)$$

$$G_{\text{eff}}/G = \xi = \frac{1}{1-p} \quad (\text{for } r_2 = 1). \quad (82)$$

For $p = 1$ [30] both G_{eff}/G and ξ diverge at the de Sitter solution. In this case one has $G_{\text{eff}}/G = \xi \simeq 1 + 4qr_2/(10q + 3)$ in the regime $r_2 \ll 1$, so that G_{eff}/G and ξ are larger than 1 for $q > 0$. The property that ξ is as large as G_{eff}/G leads to the enhancement of the effective gravitational potential relative to the matter perturbation δ_m normalized by a [30]. This gives rise to the anti-correlation between the late-time ISW effect and the LSS. Then the parameter q is constrained to be $q > 4.2 \times 10^3$ at the 95 % confidence level [38], which means that w_{DE} is very close to -1 along the tracker.

The situation is different for $\alpha \neq 0$ and $\beta \neq 0$. Let us consider the models with $p = 1$ and $q = 5/2$, i.e. $s = 0.2$, in which case the models are compatible with the observational constraints discussed in Sec. III. In the regime $r_2 \ll 1$, Eqs. (77) and (78) read

$$G_{\text{eff}}/G \simeq 1 + \frac{48411\alpha^2 - 3\alpha(3560 + 60291\beta) + 22(50 + 924\beta + 7641\beta^2)}{10(308 - 1536\alpha + 3201\beta)} r_2, \quad (83)$$

$$\xi \simeq 1 + \frac{75276\alpha^2 - 3\alpha(8020 + 99981\beta) + 22[100 + 3\beta(733 + 4527\beta)]}{20(308 - 1536\alpha + 3201\beta)} r_2. \quad (84)$$

At the de Sitter solution Eq. (80) gives

$$G_{\text{eff}}/G = \xi = \frac{1}{9(\alpha - 2\beta)}. \quad (85)$$

In Ref. [36] the authors clarified the viable parameter region in which the ghosts and Laplacian instabilities of scalar and tensor perturbations are absent. In Fig. 4 we plot the allowed parameter space in the (α, β) plane for

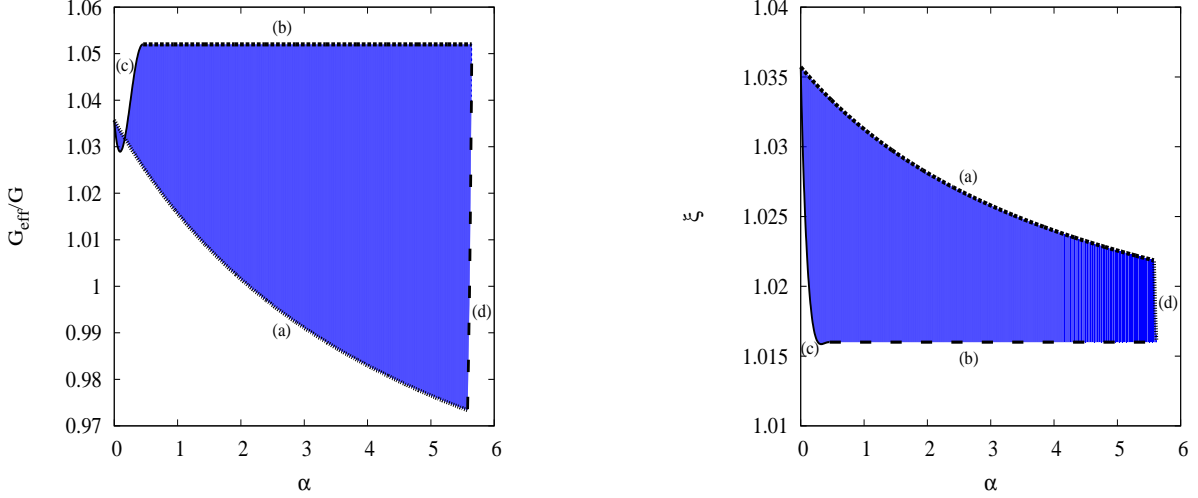


Figure 5. The left and right panels show the values of G_{eff}/G and $\xi = (G_{\text{eff}}/G)(1 + \eta)/2$ versus α for $p = 1$ and $q = 5/2$, respectively, along the tracker solution ($r_1 = 1$) at $r_2 = 0.1$. The blue regions illustrate the viable parameter spaces in which the parameters α and β belong to the blue region in Fig. 4. The borders (a), (b), (c), (d) correspond to those given in Fig. 4.

$p = 1$ and $q = 5/2$. The viable region is surrounded by the four borders: (a) $\beta = \alpha/2$, (b) $\beta = \alpha/2 - 1/15$, (c) $\beta = (408\alpha + 68 - 2\sqrt{17}\sqrt{3(272 - 75\alpha)\alpha + 68})/561$, and (d) $\beta = (242 - 15\alpha + 4\sqrt{3630 - 495\alpha})/99$. The model with $\alpha = \beta = 0$ is on the border lines [the intersection of the lines (a) and (c)], in which case both G_{eff}/G and ξ diverge at the de Sitter solution.

Figure 5 illustrates the regions for the possible values of G_{eff}/G in Eq. (83) and ξ in Eq. (84) for $p = 1$ and $q = 5/2$ at $r_2 = 0.1$. The blue regions are surrounded by the borders (a), (b), (c), (d), which correspond to those given in Fig. 4 respectively. The lines (a) in Fig. 5 show G_{eff}/G and ξ for $\beta = \alpha/2$, along which both G_{eff}/G and ξ decrease for larger α . One has $G_{\text{eff}}/G = \xi = 1.035$ for $\alpha = \beta = 0$, in which case our numerical simulations show that there is an anti-correlation between δ_m/a and Φ_{eff} for the modes deep inside the horizon. When $\alpha > 0$ the variable ξ is larger than G_{eff}/G on the line (a) for the same α , so that the anti-correlation tends to be even stronger than that for $\alpha = 0$.

On the line (b) in Fig. 4, i.e. $\beta = \alpha/2 - 1/15$, one has $G_{\text{eff}}/G \simeq 1 + 0.52r_2$ and $\xi = 1 + 0.16r_2$, which are independent of the values of α . The fact that G_{eff}/G is larger than ξ may imply the absence of the anti-correlation between δ_m/a and Φ_{eff} . In fact we will show in Sec. IV C that the anti-correlation tends to disappear as the model parameters approach the border line (b) in Fig. 4. For given α , as we move from $\beta = \alpha/2$ to $\beta = \alpha/2 - 1/15$, G_{eff}/G increases whereas ξ gets smaller. For $0 \leq \alpha \leq 34/75$ the viable regions for G_{eff}/G and ξ in Fig. 5 are surrounded by the lines (a), (c), and $\alpha = 34/75$, whereas for $5.579 \leq \alpha \leq 5.646$ they are surrounded by the lines (b), (d), and $\alpha = 5.579$.

In Fig. 6 we plot $G_{\text{eff}}/G = \xi = 1/[9(\alpha - 2\beta)]$ for the late-time de Sitter solution. Both G_{eff}/G and ξ diverge on the line (a) in Fig. 4, including the case $\alpha = \beta = 0$. On the line (b) one has $G_{\text{eff}}/G = \xi = 5/6$, so that the growth rate of matter perturbations is smaller than that in the Λ CDM model around the future de Sitter solution. The allowed values of G_{eff}/G and ξ exist in the wide regions in Fig. 6.

The present epoch corresponds to the regime between $r_2 \ll 1$ and $r_2 = 1$, so we need to resort to numerical simulations to estimate the growth rate of perturbations accurately.

C. Numerical simulations

In order to study the evolution of perturbations for a number of different wave numbers (both sub-horizon and super-horizon modes), we shall solve the full perturbation equations numerically without using the quasi-static approximation. Let us introduce the following dimensionless variables

$$V \equiv H v, \quad \delta\varphi \equiv \delta\phi/(x_{\text{dS}} M_{\text{pl}}), \quad (86)$$

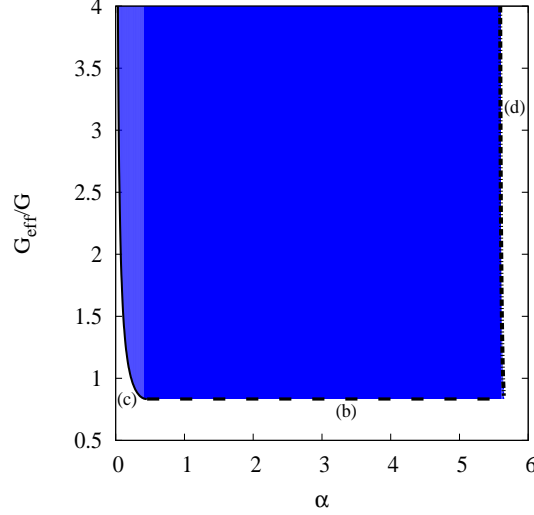


Figure 6. G_{eff}/G versus α for $p = 1$ and $q = 5/2$ at the de Sitter solution ($r_1 = 1, r_2 = 1$). Note that the parameter ξ is exactly the same as G_{eff}/G . G_{eff}/G diverges at $\beta = \alpha/2$, so that it is unbounded from above. The borders (b), (c), (d) correspond to those given in Fig. 4, respectively.

with $\tilde{A}_1 \equiv A_1/(HM_{\text{pl}}^2)$, $\tilde{A}_2 \equiv x_{\text{dS}}A_2/(HM_{\text{pl}})$, $\tilde{A}_3 \equiv A_3/M_{\text{pl}}^2$, $\tilde{A}_4 \equiv A_4/(H^2M_{\text{pl}}^2)$, $\tilde{A}_6 \equiv x_{\text{dS}}A_6/M_{\text{pl}}$, $\tilde{B}_6 \equiv B_6/M_{\text{pl}}^2$, $\tilde{B}_7 \equiv x_{\text{dS}}B_7/M_{\text{pl}}$, and $\tilde{C}_4 \equiv x_{\text{dS}}C_4/(HM_{\text{pl}})$. From Eqs. (53), (54), (55), (57), and (58) we obtain

$$\Psi = -(\tilde{B}_6\Phi + \tilde{B}_7\delta\varphi)/\tilde{A}_3, \quad (87)$$

$$\begin{aligned} \Phi' = & [(3\tilde{A}_4\tilde{A}_6\tilde{B}_6 + \tilde{A}_1\tilde{A}_2\tilde{B}_6 - 3\tilde{A}_3^2\tilde{A}_6k^2/(aH)^2 - 9\tilde{A}_6\tilde{B}_6\Omega_m)\Phi \\ & + (3\tilde{A}_2\tilde{A}_3\tilde{C}_4 + 3\tilde{A}_4\tilde{A}_6\tilde{B}_7 + \tilde{A}_1\tilde{A}_2\tilde{B}_7 - 9\tilde{A}_6\tilde{B}_7\Omega_m - 3\tilde{A}_3\tilde{A}_6^2k^2/(aH)^2)\delta\varphi + 9\tilde{A}_3\tilde{A}_6\Omega_m\delta + 9\tilde{A}_2\tilde{A}_3\Omega_mV] \\ & \times [3\tilde{A}_3(\tilde{A}_1\tilde{A}_6 - \tilde{A}_2\tilde{A}_3)]^{-1}, \end{aligned} \quad (88)$$

$$\begin{aligned} \delta\varphi' = & -[(\tilde{A}_1^2\tilde{B}_6 + 3\tilde{A}_3\tilde{A}_4\tilde{B}_6 - 3\tilde{A}_3^3k^2/(aH)^2 - 9\tilde{A}_3\tilde{B}_6\Omega_m)\Phi \\ & + (\tilde{A}_1^2\tilde{B}_7 + 3\tilde{A}_3\tilde{A}_4\tilde{B}_7 + 3\tilde{A}_1\tilde{A}_3\tilde{C}_4 - 3\tilde{A}_3^2\tilde{A}_6k^2/(aH)^2 - 9\tilde{A}_3\tilde{B}_7\Omega_m)\delta\varphi + 9\tilde{A}_3^2\Omega_m\delta + 9\tilde{A}_1\tilde{A}_3\Omega_mV] \\ & \times [3\tilde{A}_3(\tilde{A}_1\tilde{A}_6 - \tilde{A}_2\tilde{A}_3)]^{-1}, \end{aligned} \quad (89)$$

$$\delta' = -3\Phi' - k^2/(aH)^2 V, \quad (90)$$

$$V' = (H'/H)V + \Psi. \quad (91)$$

In order to recover the General Relativistic behavior in the early cosmological epoch we choose the initial conditions $\Phi' = 0$, $\delta\varphi' = 0$, $\delta\varphi = 0$, and $\delta = 10^{-5}$, in which case Φ_i , Ψ_i , and V_i are known from Eq. (87)-(89) (where the subscript “ i ” represents the initial values). For non-zero initial values of $\delta\varphi$ the field perturbation oscillates at the early stage. For the initial conditions with $|\delta\varphi_i| \lesssim |\Psi_i|$ the evolution of perturbations in the low-redshift regime is hardly affected by the oscillations. This situation is similar to that found in Ref. [30] for the model with $\alpha = \beta = 0$.

In Fig. 7 we plot the evolution of δ_m/a and Φ_{eff} versus the redshift $z = 1/a - 1$ for $p = 1$, $q = 5/2$, $\alpha = 3$, and $\beta = 1.49$ with several different wave numbers. In this case the model parameters are close to the border line (a) in Fig. 4. The solid curve in Fig. 7 corresponds to the simulation for the wave number $k = 300 a_0 H_0 \simeq 0.1 h \text{ Mpc}^{-1}$, where the subscript “0” represents the today’s values. The numerical results of δ_m/a and Φ_{eff} show good agreement with those derived under the quasi-static approximation on sub-horizon scales. For the model parameters used in Fig. 7 the analytic estimates (83) and (84) give $G_{\text{eff}}/G \simeq 1 - 0.05r_2$ and $\xi \simeq 1 + 0.23r_2$ in the regime $r_2 \ll 1$, whereas from Eq. (85) one has $G_{\text{eff}}/G = \xi = 5.56$ at the de Sitter solution. From Fig. 7 we find that δ_m/a is anti-correlated with Φ_{eff} for the modes $k \gg a_0 H_0$. This property comes from the fact that the parameter ξ is always larger than 1, while G_{eff}/G is smaller than ξ in the regime $r_2 \ll 1$. In Fig. 7 the growth rates of δ_m and Φ_{eff} decrease for smaller k . The anti-correlation between δ_m/a and Φ_{eff} is present for the modes $k \gtrsim 5a_0 H_0$.

Figure 8 shows the evolution of δ_m/a and Φ_{eff} for $p = 1$, $q = 5/2$, $\alpha = 3$, and $\beta = 1.45$ with several different wave numbers. In this case β is smaller than that used in Fig. 7. From Eqs. (83) and (84) one has $G_{\text{eff}}/G = 1 + 0.25r_2$ and $\xi = 1 + 0.16r_2$ for $r_2 \ll 1$, whereas $G_{\text{eff}} = \xi = 1.11$ at the de Sitter solution. Compared to the case $\beta = 1.49$, G_{eff}/G and ξ get larger and smaller, respectively, for the same value of r_2 ($\ll 1$). This leads to the suppression of the growth of Φ_{eff} . From Fig. 8 we find that δ_m/a and Φ_{eff} are positively correlated for the mode $k = 300a_0 H_0$. For the

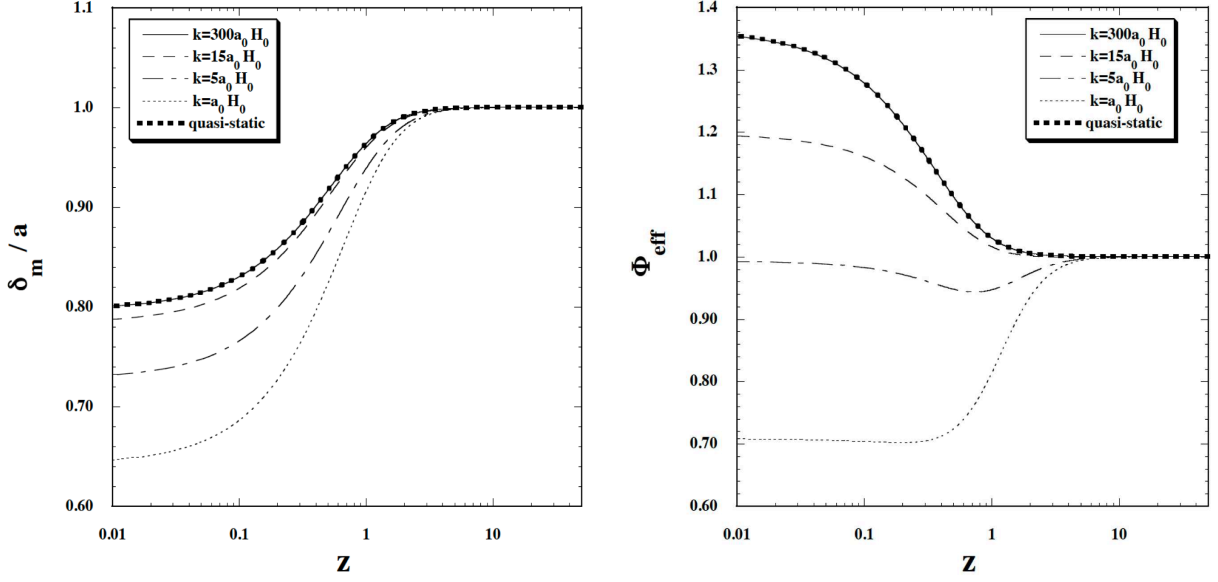


Figure 7. Evolution of δ_m/a (left) and Φ_{eff} (right) versus the redshift z for $p = 1$, $q = 5/2$, $\alpha = 3$, $\beta = 1.49$ along the tracker solution. Note that δ_m/a and Φ_{eff} are normalized by their initial values, respectively. Each curve corresponds to the evolution of perturbations for the wave numbers $k = 300a_0H_0$, $k = 15a_0H_0$, $k = 5a_0H_0$, and $k = a_0H_0$. The dotted curves show the results obtained under the quasi-static approximation on sub-horizon scales. In this case there is an anti-correlation between δ_m/a and Φ_{eff} for the modes $k \gtrsim 5a_0H_0$.

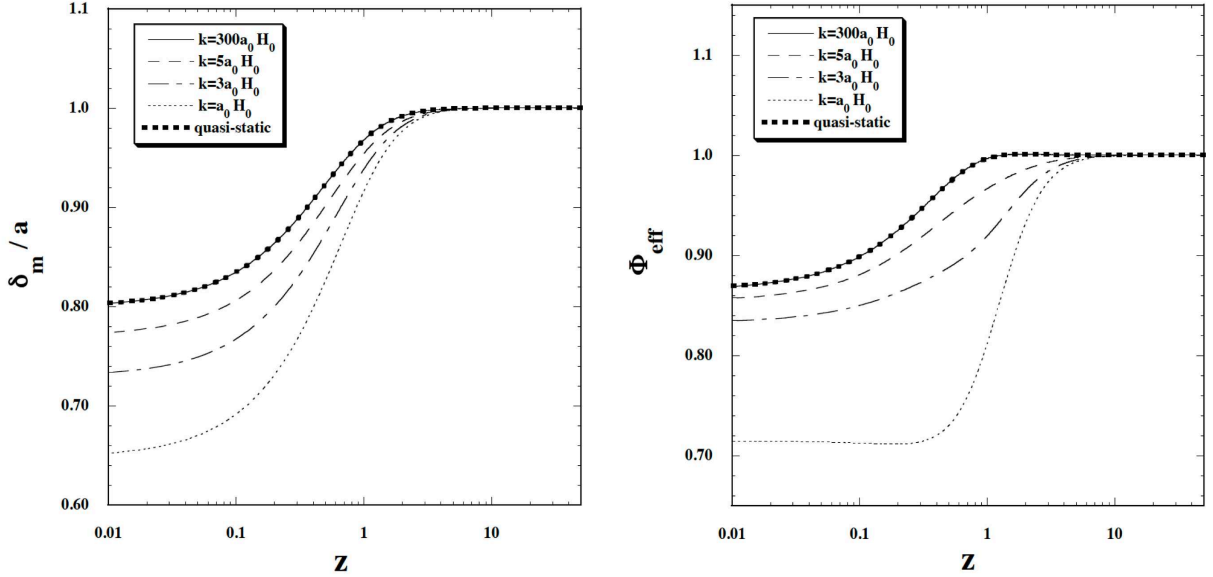


Figure 8. Similar to Fig. 7, but for the model parameters $p = 1$, $q = 5/2$, $\alpha = 3$, $\beta = 1.45$. In this case δ_m/a and Φ_{eff} are not anti-correlated.

wave numbers $k \gg a_0H_0$ the quasi-static approximation reproduces the numerical results in high accuracy. On larger scales both δ_m and Φ_{eff} evolve more slowly, so that δ_m/a and Φ_{eff} are also positively correlated.

We define growth index γ of matter perturbations, as [51]

$$\frac{\dot{\delta}_m}{H\delta_m} = (\Omega_m)^\gamma. \quad (92)$$

In the Λ CDM model $\gamma \simeq 0.55$ for the redshift $0 \leq z \lesssim 1$ [52]. In Fig. 9 we plot the evolution of γ for $p = 1$ and $q = 5/2$ with the wave number $k = 300a_0H_0$ in three different cases: (i) $\alpha = 3$, $\beta = 1.49$, (ii) $\alpha = 3$, $\beta = 1.45$, and

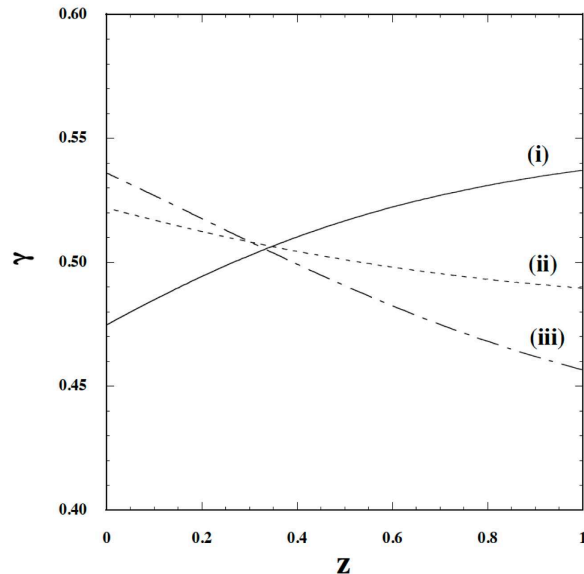


Figure 9. Evolution of the growth index γ for the mode $k = 300a_0H_0$ in the regime $0 < z < 1$ with the model parameters (i) $p = 1$, $q = 5/2$, $\alpha = 3$, $\beta = 1.49$, (ii) $p = 1$, $q = 5/2$, $\alpha = 3$, $\beta = 1.45$, and (iii) $p = 1$, $q = 5/2$, $\alpha = 3$, $\beta = 1.434$.

(iii) $\alpha = 3$, $\beta = 1.434$. The numerical simulations for (i) and (ii) correspond to the model parameters used in Figs. 7 and 8, respectively, whereas the model parameter in the case (iii) is close to the border (b) in Fig. 4. In the cases (i), (ii), (iii) the effective gravitational couplings in the regime $r_2 \ll 1$ are $G_{\text{eff}}/G = 1 - 0.05r_2$, $G_{\text{eff}}/G = 1 + 0.26r_2$, $G_{\text{eff}}/G = 1 + 0.51r_2$, respectively, whereas at the de Sitter solution $G_{\text{eff}}/G = 5.56$, $G_{\text{eff}}/G = 1.11$, $G_{\text{eff}}/G = 0.84$, respectively. For smaller β , G_{eff} is larger in the early epoch ($r_2 \ll 1$), so that the deviation of γ from the value 0.55 is more significant. On the other hand, G_{eff} at the de Sitter solution gets smaller for decreasing β , which leads to the approach to the value 0.55 around $z = 0$.

While the above discussion corresponds to the case $s = 0.2$, we have also studied the evolution of perturbations for different values of s and found the similar properties to those discussed above. For $p = 1$ the upper bound for the allowed parameter space in the (α, β) plane is characterized by the line $\beta = \alpha/2$ [36], around which the ISW-LSS anti-correlation is present for $0 < s < 0.36$ (i.e. for s constrained observationally at the background level). As β gets smaller for a fixed α (> 0), the anti-correlation tends to disappear. We also found that, for $p = 1$ and $0 < s < 0.36$, the growth index γ varies in the range $0.4 \lesssim \gamma \lesssim 0.6$ for $0 \leq z \lesssim 1$. The ISW-LSS anti-correlation as well the variation of γ allows us to discriminate between the extended Galileon models and the Λ CDM.

V. CONCLUSIONS

In this paper we have studied cosmological constraints on the extended Galileon models of dark energy. For the functions (7) with the powers (8) there exist tracker solutions along which the field equation of state w_{DE} changes as $-1 - 4s/3$ (radiation era) $\rightarrow -1 - s$ (matter era) $\rightarrow -1$ (de Sitter era), where $s = p/(2q) > 0$. Unlike the case of the covariant Galileon ($s = 1$), w_{DE} can be close to -1 during the radiation and matter eras for $0 \leq s \ll 1$. Moreover, even for $w_{\text{DE}} < -1$, there are viable model parameter spaces in which the ghosts and Laplacian instabilities are absent.

Using the recent data of SN Ia, CMB, and BAO, we placed observational constraints on the background tracker solutions with $s > 0$. In the flat Universe we found that the model parameters are constrained to be $s = 0.034^{+0.327}_{-0.034}$ and $\Omega_{m,0} = 0.271^{+0.024}_{-0.010}$ (95% CL) from the joint data analysis. The chi-square for the best-fit case ($s = 0.034$) is slightly smaller than that in Λ CDM. However the difference of the AIC information criteria between the two models is $\Delta(\text{AIC}) = 1.85$, so that the extended Galileon is not particularly favored over the Λ CDM. We also carried out the likelihood analysis in the presence of the cosmic curvature K and obtained the bounds $s = 0.067^{+0.333}_{-0.067}$, $\Omega_{m,0} = 0.277^{+0.023}_{-0.022}$, and $\Omega_{K,0} = 0.0077^{+0.0039}_{-0.0127}$ (95% CL). The tracker for the covariant Galileon ($s = 1$) is disfavored from the data, in which case only the late-time tracking solution is allowed observationally [31].

The background quantities for the tracker are independent of the values of α and β . This means that the models

with different α and β cannot be distinguished from the observational constraints derived from the background cosmic expansion history. In order to break this degeneracy we studied the evolution of cosmological perturbations in the presence of non-relativistic matter for the flat FLRW background. As shown in Ref. [30], for $\alpha = \beta = 0$, the matter density perturbation δ_m divided by the scale factor a is anti-correlated with the effective gravitational potential Φ_{eff} for the modes relevant to the LSS. This leads to the anti-correlation between the LSS and the ISW effect in CMB, so that the parameter s for the tracker is severely constrained to be $s < 1.2 \times 10^{-4}$ (95% CL).

For the models with $\alpha \neq 0$ and $\beta \neq 0$, however, the correlation between δ_m/a and Φ_{eff} depends on the values of α and β . If $p = 1$ and $q = 5/2$ (i.e. $s = 0.2$), for example, δ_m/a and Φ_{eff} tend to be positively correlated for the model parameters close to the border (b) in Fig. 4 ($\beta = \alpha/2 - 1/15$), whereas they show anti-correlations for α and β close to the border (a) ($\beta = \alpha/2$). The typical examples of the positive and negative correlations are plotted in Figs. 8 and 7, respectively. The qualitative differences between these two cases can be understood by estimating the effective gravitational coupling G_{eff} and the quantity $\xi = (G_{\text{eff}}/G)(1 + \eta)/2$ derived under the quasi-static approximation on sub-horizon scales. As the model parameters approach the border (a) in Fig. 4, ξ gets larger while G_{eff} decreases, so that the anti-correlation between δ_m/a and Φ_{eff} tends to be stronger. We studied the evolution of perturbations for different values of s in the range $0 < s < 0.36$ and found that the basic properties for the ISW-LSS correlation are similar to those discussed for $s = 0.2$.

We also estimated the growth index γ of the matter perturbation and found that, for $p = 1$ and $0 < s < 0.36$, it typically varies in the range $0.4 \lesssim \gamma \lesssim 0.6$ at the redshifts for $0 \leq z \lesssim 1$. Hence it is also possible to distinguish between the extended Galileon models and the Λ CDM model from the galaxy clustering. However, we expect that the tightest observational bounds on the values α and β should come from the ISW-LSS correlation. We leave such observational constraints for future works.

ACKNOWLEDGEMENTS

We thank Savvas Nesseris for providing us a related numerical code for the likelihood analysis of CMB, BAO, and SN Ia. The work of A. D. F. and S. T. was supported by the Grant-in-Aid for Scientific Research Fund of the JSPS Nos. 10271 and 30318802. S. T. also thanks financial support for the Grant-in-Aid for Scientific Research on Innovative Areas (No. 21111006).

-
- [1] W. J. Percival *et al.*, Mon. Not. Roy. Astron. Soc. **401**, 2148 (2010).
 - [2] A. G. Riess *et al.*, Astrophys. J. **699**, 539 (2009).
 - [3] E. Komatsu *et al.* [WMAP Collaboration], Astrophys. J. Suppl. **192**, 18 (2011).
 - [4] M. Chevallier and D. Polarski, Int. J. Mod. Phys. D **10**, 213 (2001); E. V. Linder, Phys. Rev. Lett. **90**, 091301 (2003).
 - [5] Y. Wang, Phys. Rev. D **80**, 123525 (2009); A. Vikhlinin *et al.*, Astrophys. J. **692**, 1060 (2009).
 - [6] Y. Fujii, Phys. Rev. D **26**, 2580 (1982); L. H. Ford, Phys. Rev. D **35**, 2339 (1987); C. Wetterich, Nucl. Phys. B. **302**, 668 (1988); B. Ratra and J. Peebles, Phys. Rev. D **37**, 321 (1988); T. Chiba, N. Sugiyama and T. Nakamura, Mon. Not. Roy. Astron. Soc. **289**, L5 (1997); P. G. Ferreira and M. Joyce, Phys. Rev. Lett. **79**, 4740 (1997); R. R. Caldwell, R. Dave and P. J. Steinhardt, Phys. Rev. Lett. **80**, 1582 (1998).
 - [7] R. R. Caldwell, Phys. Lett. B **545**, 23 (2002); P. Singh, M. Sami and N. Dadhich, Phys. Rev. D **68**, 023522 (2003); M. P. Dabrowski, T. Stachowiak and M. Szydlowski, Phys. Rev. D **68**, 103519 (2003); M. Sami and A. Toporensky, Mod. Phys. Lett. A **19**, 1509 (2004); Z. K. Guo, Y. S. Piao, X. M. Zhang and Y. Z. Zhang, Phys. Lett. B **608**, 177 (2005); M. z. Li, B. Feng and X. m. Zhang, JCAP **0512**, 002 (2005); H. Wei, R. G. Cai and D. F. Zeng, Class. Quant. Grav. **22**, 3189 (2005).
 - [8] S. M. Carroll, M. Hoffman and M. Trodden, Phys. Rev. D **68**, 023509 (2003); J. M. Cline, S. Jeon and G. D. Moore, Phys. Rev. D **70**, 043543 (2004).
 - [9] E. J. Copeland, M. Sami, S. Tsujikawa, Int. J. Mod. Phys. **D15**, 1753-1936 (2006); K. Koyama, Class. Quant. Grav. **24**, R231-R253 (2007); R. Durrer and R. Maartens, Gen. Rel. Grav. **40**, 301-328 (2008); T. P. Sotiriou and V. Faraoni, Rev. Mod. Phys. **82**, 451 (2010); A. De Felice and S. Tsujikawa, Living Rev. Rel. **13**, 3 (2010); S. Tsujikawa, Lect. Notes Phys. **800**, 99-145 (2010); T. Clifton, P. G. Ferreira, A. Padilla and C. Skordis, arXiv:1106.2476 [astro-ph.CO].
 - [10] W. Hu and I. Sawicki, Phys. Rev. D **76**, 064004 (2007).
 - [11] L. Amendola and S. Tsujikawa, Phys. Lett. B **660**, 125 (2008).
 - [12] S. Tsujikawa, Phys. Rev. D **77**, 023507 (2008).
 - [13] H. Motohashi, A. A. Starobinsky and J. Yokoyama, Prog. Theor. Phys. **123**, 887 (2010).
 - [14] L. Amendola, R. Gannouji, D. Polarski and S. Tsujikawa, Phys. Rev. D **75**, 083504 (2007); A. A. Starobinsky, JETP Lett. **86**, 157 (2007); S. A. Appleby and R. A. Battye, Phys. Lett. B **654**, 7 (2007); E. V. Linder, Phys. Rev. **D80**, 123528 (2009).
 - [15] C. Brans and R. H. Dicke, Phys. Rev. **124**, 925 (1961).

- [16] J. Khoury and A. Weltman, Phys. Rev. Lett. **93**, 171104 (2004); Phys. Rev. **D69**, 044026 (2004).
- [17] S. Tsujikawa, K. Uddin, S. Mizuno, R. Tavakol and J. Yokoyama, Phys. Rev. **D77**, 103009 (2008).
- [18] R. Gannouji, B. Moraes, D. F. Mota, D. Polarski, S. Tsujikawa, and H. A. Winther, Phys. Rev. **D82**, 124006 (2010).
- [19] A. I. Vainshtein, Phys. Lett. B **39**, 393 (1972).
- [20] G. R. Dvali, G. Gabadadze and M. Porrati, Phys. Lett. **B485**, 208-214 (2000).
- [21] A. Nicolis, R. Rattazzi and E. Trincherini, Phys. Rev. **D79**, 064036 (2009).
- [22] C. Deffayet, G. R. Dvali, G. Gabadadze and A. I. Vainshtein, Phys. Rev. D **65**, 044026 (2002); M. Porrati, Phys. Lett. B **534**, 209 (2002).
- [23] E. Babichev, C. Deffayet and R. Ziour, Int. J. Mod. Phys. D **18**, 2147 (2009); R. Gannouji and M. Sami, Phys. Rev. **D82**, 024011 (2010); E. Babichev, C. Deffayet and G. Esposito-Farese, Phys. Rev. D **84**, 061502 (2011); N. Kaloper, A. Padilla and N. Tanahashi, JHEP **1110**, 148 (2011); A. De Felice, R. Kase and S. Tsujikawa, arXiv:1111.5090 [gr-qc]; R. Kimura, T. Kobayashi and K. Yamamoto, arXiv:1111.6749 [astro-ph.CO].
- [24] C. Deffayet, G. Esposito-Farese and A. Vikman, Phys. Rev. **D79**, 084003 (2009); C. Deffayet, S. Deser and G. Esposito-Farese, Phys. Rev. D **80**, 064015 (2009); C. de Rham and A. J. Tolley, JCAP **1005**, 015 (2010).
- [25] N. Chow and J. Khoury, Phys. Rev. **D80**, 024037 (2009); F. P. Silva and K. Koyama, Phys. Rev. D **80**, 121301 (2009); T. Kobayashi, H. Tashiro and D. Suzuki, Phys. Rev. D **81**, 063513 (2010); T. Kobayashi, Phys. Rev. **D81**, 103533 (2010); A. Ali, R. Gannouji and M. Sami, Phys. Rev. **D82**, 103015 (2010); D. F. Mota, M. Sandstad and T. Zlosnik, JHEP **1012**, 051 (2010); A. De Felice and S. Tsujikawa, JCAP **1007**, 024 (2010); A. De Felice, S. Mukohyama and S. Tsujikawa, Phys. Rev. **D82**, 023524 (2010); K. Hirano and Z. Komiya, arXiv:1012.5451 [astro-ph.CO]; O. Pujolas, I. Sawicki and A. Vikman, arXiv:1103.5360 [hep-th]; C. de Rham and L. Heisenberg, Phys. Rev. **D84**, 043503 (2011).
- [26] T. Kobayashi, M. Yamaguchi and J. Yokoyama, Phys. Rev. Lett. **105**, 231302 (2010); C. Burrage, C. de Rham, D. Seery and A. J. Tolley, JCAP **1101**, 014 (2011); S. Mizuno and K. Koyama, Phys. Rev. **D82**, 103518 (2010); K. Hinterbichler, M. Trodden and D. Wesley, Phys. Rev. D **82**, 124018 (2010); P. Creminelli, G. D'Amico, M. Musso, J. Norena and E. Trincherini, JCAP **1102**, 006 (2011); A. Naruko and M. Sasaki, Class. Quant. Grav. **28**, 072001 (2011); A. De Felice and S. Tsujikawa, JCAP **1104**, 029 (2011); T. Kobayashi, M. Yamaguchi and J. Yokoyama, Phys. Rev. **D83**, 103524 (2011); G. Goon, K. Hinterbichler and M. Trodden, JCAP **1112**, 004 (2011); X. Gao and D. A. Steer, arXiv:1107.2642 [astro-ph.CO]; A. De Felice and S. Tsujikawa, Phys. Rev. **D84**, 083504 (2011).
- [27] A. De Felice and S. Tsujikawa, Phys. Rev. Lett. **105**, 111301 (2010).
- [28] A. De Felice and S. Tsujikawa, arXiv:1008.4236 [hep-th] (Physical Review D to appear).
- [29] C. Deffayet, O. Pujolas, I. Sawicki and A. Vikman, JCAP **1010**, 026 (2010).
- [30] R. Kimura and K. Yamamoto, JCAP **1104**, 025 (2011).
- [31] S. Nesseris, A. De Felice and S. Tsujikawa, Phys. Rev. **D82**, 124054 (2010).
- [32] C. Deffayet, X. Gao, D. A. Steer and G. Zahariade, Phys. Rev. **D84**, 064039 (2011).
- [33] G. W. Horndeski, Int. J. Theor. Phys. **10**, 363-384 (1974).
- [34] T. Kobayashi, M. Yamaguchi and J. Yokoyama, Prog. Theor. Phys. **126**, , 511-529 (2011).
- [35] C. Charmousis, E. J. Copeland, A. Padilla and P. M. Saffin, arXiv:1106.2000 [hep-th].
- [36] A. De Felice and S. Tsujikawa, arXiv:1110.3878 [gr-qc].
- [37] G. Dvali and M. S. Turner, astro-ph/0301510.
- [38] R. Kimura, T. Kobayashi and K. Yamamoto, arXiv:1110.3598 [astro-ph.CO].
- [39] M. Hicken *et al.*, Astrophys. J. **700**, 1097 (2009).
- [40] W. Hu and N. Sugiyama, Astrophys. J. **471**, 542 (1996).
- [41] J. R. Bond, G. Efstathiou and M. Tegmark, Mon. Not. Roy. Astron. Soc. **291**, L33 (1997); Y. Wang and P. Mukherjee, Phys. Rev. D **76**, 103533 (2007); H. Li *et al.*, Astrophys. J. **683**, L1 (2008); J. C. B. Sanchez, S. Nesseris and L. Perivolaropoulos, JCAP **0911**, 029 (2009).
- [42] D. J. Eisenstein and W. Hu, Astrophys. J. **496**, 605 (1998).
- [43] R. Lazkoz, S. Nesseris and L. Perivolaropoulos, JCAP **0807**, 012 (2008).
- [44] R. Amanullah *et al.*, Astrophys. J. **716**, 712 (2010).
- [45] A. R. Liddle, Mon. Not. Roy. Astron. Soc. **351**, L49 (2004).
- [46] J. M. Bardeen, Phys. Rev. D **22**, 1882 (1980).
- [47] A. De Felice, T. Kobayashi and S. Tsujikawa, Phys. Lett. B **706**, 123 (2011).
- [48] C. Schmid, J. -P. Uzan and A. Riazuelo, Phys. Rev. D **71**, 083512 (2005); L. Amendola, M. Kunz and D. Sapone, JCAP **0804**, 013 (2008).
- [49] A. A. Starobinsky, JETP Lett. **68**, 757 (1998); B. Boisseau, G. Esposito-Farese, D. Polarski and A. A. Starobinsky, Phys. Rev. Lett. **85**, 2236 (2000); G. Esposito-Farese and D. Polarski, Phys. Rev. **D63**, 063504 (2001); S. Tsujikawa, Phys. Rev. D **76**, 023514 (2007); S. Tsujikawa, K. Uddin and R. Tavakol, Phys. Rev. D **77**, 043007 (2008).
- [50] A. De Felice, R. Kase and S. Tsujikawa, Phys. Rev. **D83**, 043515 (2011).
- [51] J. Peebles, *The large-scale structure of the universe*, Princeton University Press (1980).
- [52] L. M. Wang and P. J. Steinhardt, Astrophys. J. **508**, 483 (1998); E. V. Linder, Phys. Rev. D **72**, 043529 (2005).